Nonlinear Dynamics (2006) 44: 135–149
DOI: 10.1007/s11071-006-1957-x

Synchronization Analysis of Coupled Noncoherent Oscillators

JÜRGEN KURTHS[1,*], M. CARMEN ROMANO[1], MARCO THIEL[1], GRIGORY V. OSIPOV[2], MIKHAIL V. IVANCHENKO[2], ISTVÁN Z. KISS[3], and JOHN L. HUDSON[3]
[1]*Institute of Physics, Universität Potsdam,14469 Potsdam, Germany;* [2]*Department of Radiophysics, Nizhny Novgorod University, 23, Gagarin Avenue, 603950 Nizhny Novgorod, Russia;* [3]*Department of Chemical Engineering, 102 Engineers Way, University of Virginia, Charlottesville, VA 22904-479, U.S.A.* *Author for correspondence (e-mail: *juergen@agnld.uni-potsdam.de)*

(Received: 20 September 2004; accepted: 14 March 2005)

Abstract. We present two different approaches to detect and quantify phase synchronization in the case of coupled non-phase coherent oscillators. The first one is based on the general idea of curvature of an arbitrary curve. The second one is based on recurrences of the trajectory in phase space. We illustrate both methods in the paradigmatic example of the Rössler system in the funnel regime. We show that the second method is applicable even in the case of noisy data. Furthermore, we extend the second approach to the application of chains of coupled systems, which allows us to detect easily clusters of synchronized oscillators. In order to illustrate the applicability of this approach, we show the results of the algorithm applied to experimental data from a population of 64 electrochemical oscillators.

Key words: chaotic oscillators, data analysis, synchronization

1. Introduction

Phase synchronization has been studied extensively during the last years [1–4], as this phenomenon has found numerous applications in natural [5–10] and engineering systems [11–13]. Two systems are said to be phase synchronized when their respective frequencies and phases are locked. Till now chaotic phase synchronization (CPS) has been mainly observed for chaotic attractors with rather coherent phase dynamics. These attractors have a relatively simple topology of oscillations and a well-pronounced peak in the power spectrum, which allows us to introduce the phase and the characteristic frequency of motions. However, some difficulties appear dealing with non-coherent attractors with a rather broad band power spectra. Then it might not be straightforward to define a phase of the oscillations, and in general no single characteristic time scale exists. In contrast to phase coherent attractors, it is quite unclear whether some phase synchronized state can be achieved. To treat this problem, we propose in this paper two different approaches: (i) we present a method that defines the phase more generally and allows us to study CPS in systems of coupled chaotic oscillators with even strongly noncoherent phase properties and (ii) we propose a method based on recurrences in phase space, that allows us to quantify indirectly CPS, which even works in the case of noisy noncoherent oscillators. We demonstrate the applicability of both methods for the paradigmatic system of two coupled nonidentical Rössler oscillators:

$$\begin{aligned} \dot{x}_{1,2} &= -\omega_{1,2} y_{1,2} - z_{1,2}, \\ \dot{y}_{1,2} &= \omega_{1,2} x_{1,2} + a y_{1,2} + \mu(y_{2,1} - y_{1,2}), \\ \dot{z}_{1,2} &= 0.1 + z_{1,2}(x_{1,2} - 8.5), \end{aligned} \tag{1}$$

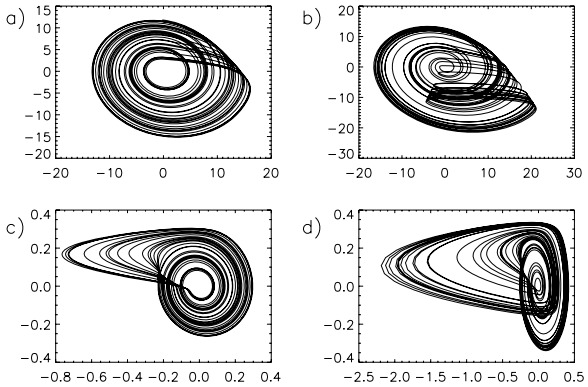

Figure 1. Upper panel (a),(b): projections of the attractors of the Rössler systems (1) onto the plane (x, y); lower panel (c),(d): projections onto $(\dot{x}, \dot{y})$. The parameters are $\omega = 1.02$ and $a = 0.16$ (a),(c), resp. $a = 0.2925$ (b), (d)

where μ is the coupling strength. $\omega_{1,2}$ determine the mean frequency of the oscillators in the case of phase coherent attractors. In our simulations we take $\omega_1 = 0.98$ and $\omega_2 = 1.02$. The parameter $a \in [0.15 : 0.3]$ governs the topology of the chaotic attractor. When a is below a critical value a_c ($a_c \approx 0.186$ for $\omega_1 = 0.98$ and $a_c \approx 0.195$ for $\omega_2 = 1.02$), the chaotic trajectories always cycle around the unstable fixed point $(x_0, y_0) \approx (0, 0)$ in the (x, y) subspace, i.e., $\max(y) > y_0$ (Figure 1a). In this case, the rotation angle

$$\phi = \arctan \frac{y}{x} \tag{2}$$

can be defined as the phase, which increases almost uniformly, i.e., the oscillator has a coherent phase dynamics. Beyond the critical value a_c, the trajectories no longer always completely cycle around (x_0, y_0), and some $\max(y) < y_0$ occur, which are associated with faster returns of the orbits; the attractor becomes a funnel one. Such earlier returns in the funnel attractor happen more frequently with increasing a (Figure 1b). It is clear that for the funnel attractors, usual (and rather simple) definitions of phase, such as Equation (2) [1–4], are no longer applicable.

2. Phase calculation basing on curvature

In order to overcome the problem of the definition of the phase in the case of noncoherent oscillators, we firstly propose another approach which is based on the general idea of the curvature of an arbitrary curve [14]. For any two-dimensional curve $\vec{r}_1 = (u, v)$ the angle velocity at each point is $\nu = \frac{ds}{dt}/R$, where $ds/dt = \sqrt{\dot{u}^2 + \dot{v}^2}$ is the speed along the curve and $R = (\dot{u}^2 + \dot{v}^2)^{3/2}/[\dot{v}\ddot{u} - \ddot{v}\dot{u}]$ is the radius of the curvature. If $R > 0$ at each point, then $\nu = \frac{d\phi}{dt} = \frac{\dot{v}\ddot{u} - \ddot{v}\dot{u}}{\dot{u}^2 + \dot{v}^2}$ is always positive and therefore the variable ϕ defined as $\phi = \int \nu dt = \arctan \frac{\dot{v}}{\dot{u}}$, is a monotonically growing angle function of time and can be considered as a phase of the oscillations. Geometrically it means that the projection $\vec{r}_2 = (\dot{u}, \dot{v})$ is a curve cycling monotonically around a certain point.

These definitions of ϕ and ν hold in general for any dynamical system if the projection of the phase trajectory on some plane is a curve with a positive curvature. We find that it is applicable to a large variety of chaotic oscillators, such as Lorenz system [15], Chua circuit [16], the model of an ideal four-level laser with periodic pump modulation [17] or a chemical system [18].

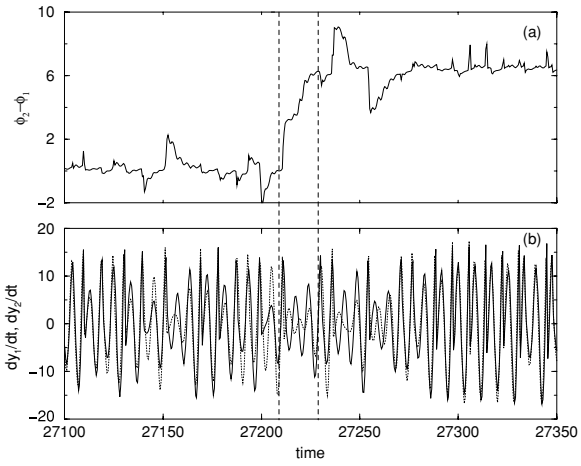

Figure 2. (a) Time evolution of phase difference of the system of EQ. (1). (b) Variables $\dot{y}_{1,2}$ in system (1) for $a = 0.2925$ and $\mu = 0.179$. Solid and dotted lines correspond to the first and the second oscillator, respectively. In the time interval between dashed lines the first oscillator produces four rotations in the $(\dot{x}_1, \dot{y}_1)$-plane around the origin, but the second one generates only three rotations, which leads to a phase slip in (a)

This is clear for phase-coherent as well as funnel attractors in the Rössler oscillator. Here projections of chaotic trajectories on the plane $(\dot{x}, \dot{y})$ always rotate around the origin (Figs. 1c and d) and the phase can be defined as

$$\phi = \arctan \frac{\dot{y}}{\dot{x}}. \tag{3}$$

We have to note that for the funnel chaotic attractors the coupling may change their topology. As a consequence the strong cyclic structure of orbits projection in the $(\dot{x}, \dot{y})$-plane may be destroyed and the phase measurement Equation (3) fails occasionally for intermediate values of coupling. But for small coupling and for coupling near the transition to CPS, the phase is well-defined by Equation (3) [19].

We use two criteria to detect the existence of CPS: locking of the mean frequencies $\Omega_1 = \langle \nu_1 \rangle = \Omega_2 = \langle \nu_2 \rangle$, and locking of the phase $|\phi_2(t) - \phi_1(t)| \leq \text{const}$ (we consider here only 1:1 synchronization). Applying the new definition of the phase Equation (3) to the system of Equation (1) for $a = 0.2925$ (strongly noncoherent) and $\mu = 0.179$, we obtain the phase difference represented in Figure 2.

We find two large plateaus in the evolution of the difference of the phases with time, i.e., we detect CPS, but we also find a phase slip associated to a different number of oscillations in the two oscillators in the represented period of time. This means, we observe the seldom occurrence of phase slips. It is interesting to note that in this system CPS occurs after one of the positive Lyapunov exponents passes to negative values, i.e., it is also a transition to generalized chaotic synchronization (GCS).

Although this approach works well in noncoherent model systems, we have to consider that one is often confronted with the computation of the phase in experimental time series, which are usually corrupted by noise. In this case, some difficulties may appear in computing the phase by Equation (3), because derivatives are involved in its definition. We will address this problem in the next section.

3. Phase synchronization by means of recurrences

Here, we propose a rather different approach based on recurrences in phase space to detect and quantify CPS. The concept of recurrence in dynamical systems goes back to Poincaré [20], when he proved

that after a sufficiently long time interval, the trajectory of an isolated mechanical system will return arbitrarily close to each former point of its route.

We define a recurrence of the trajectory of a dynamical system $\{\vec{x}_i\}_{i=1}^{N}$ in the following way: we say that the trajectory has returned at $t = j\delta t$ to the former state at $t = i\delta t$ if

$$R_{i,j}^{(\varepsilon)} = \Theta(\varepsilon - ||\vec{x}_i - \vec{x}_j||) = 1, \tag{4}$$

where ε is a pre-defined threshold, $\Theta(.)$ is the Heaviside function and δt is the sampling rate [21]. Based on this definition of recurrence, it is straightforward to estimate the probability $P^{(\varepsilon)}(\tau)$ that the system returns to the neighborhood of a former point $\vec{x}_i$ of the trajectory (the neighborhood is defined as a box of size ε centered at $\vec{x}_i$, as we use the maximum norm) after τ time steps

$$\hat{P}^{(\varepsilon)}(\tau) = \frac{1}{N-\tau}\sum_{i=1}^{N-\tau}\Theta(\varepsilon - ||\vec{x}_i - \vec{x}_{i+\tau}||) = \frac{1}{N-\tau}\sum_{i=1}^{N-\tau}R_{i,i+\tau}^{(\varepsilon)}. \tag{5}$$

This function can be considered as a generalized autocorrelation function, as it also describes higher order correlations between the points of the trajectory in dependence on the time delay τ. A further advantage with respect to the linear autocorrelation function is that $\hat{P}^{(\varepsilon)}(\tau)$ is determined for a trajectory in phase space and not only for a single observable of the system's trajectory. Further, we have recently shown that it is possible to reconstruct the attractor by only considering the recurrences of single components of the system [22]. Because of this, it is also possible to estimate dynamical invariants of the system (e.g., entropies and dimensions) by means of recurrences in phase space even without embedding [23], i.e. the recurrences of the system in phase space contain information about higher order dependencies within the components of the system. This method has been successfully applied to experimental flow [23] and geophysical data [24].

For a periodic system in phase space, it can be easily shown that $P(\tau) = \lim_{\varepsilon\to 0} P^{(\varepsilon)}(\tau)$ is equal to 1 if τ is equal to a multiple of the period T of the system, and 0 otherwise. For coherent chaotic oscillators , such as Equation (1) for $a = 0.16$, $\hat{P}^{(\varepsilon)}(\tau)$ has local maxima at multiples of the mean period, but the probability of recurrence after one or more rotations around the fixed point is less than one.

Analyzing the probability of recurrence, it is possible to detect CPS for noncoherent oscillators. This approach is based on the following idea: Originally, a phase ϕ is assigned to a periodic trajectory $\vec{x}$ in phase space, by projecting the trajectory onto a plane and choosing an origin, around which the whole trajectory oscillates. Then an increment of 2π is assigned to ϕ, when the point of the trajectory has returned to its starting position, i.e., when $\vec{y}(t+T) - \vec{y}(t) = \vec{0}$. Analogously to the case of a periodic system, we can refer an increment of 2π to ϕ to a complex non-periodic trajectory $\vec{x}(t)$, when $|\vec{x}(t+T) - \vec{x}(t)| \sim 0$, or equivalently when $|\vec{x}(t+T) - \vec{x}(t)| < \varepsilon$, where ε is a predefined threshold. That means, a recurrence $R_{t,t+\tau}^{(\varepsilon)} = 1$ can be interpreted as an increment of 2π of the phase in the time interval τ.

$\hat{P}^{(\varepsilon)}(\tau)$ can be viewed as a statistical measure on how often ϕ in the original phase space has increased by 2π or multiples of 2π within the time interval τ. If two systems are in PS, in the mean, the phases of both systems increase by $k \cdot 2\pi$, with k a natural number, within the same time interval τ. Hence, looking at the coincidence of the positions of the maxima of $\hat{P}^{(\varepsilon)}(\tau)$ for both systems, we can quantitatively identify PS (from now on, we omit (ε) and $\hat{}$ in $\hat{P}^{(\varepsilon)}(\tau)$ to simplify the notation). The proposed algorithm consists of two steps:

- Compute $P_{1,2}(\tau)$ of both systems based on Equation (5).
- Compute the cross-correlation coefficient between $P_1(\tau)$ and $P_2(\tau)$ (Correlation between Probabilities of Recurrence)

$$\mathrm{CPR}^{1,2} = \frac{\langle \bar{P}_1(\tau)\bar{P}_2(\tau)\rangle}{\sigma_1\sigma_2}, \tag{6}$$

where $\bar{P}_{1,2}$ means that the mean value has been subtracted and σ_1 and σ_2 are the standard deviations of $P_1(\tau)$ resp. $P_2(\tau)$.

If both systems are in PS, the probability of recurrence is maximal at the same time and $\mathrm{CPR}^{1,2} \sim 1$. In contrast, if the systems are not in PS, the maxima of the probability of recurrence do not occur simultaneously. Then we observe a drift (Figure 5b) and expect low values of $\mathrm{CPR}^{1,2}$.

3.1. Examples

In this section we exemplify the application of the index CPR for PS to four prototypical examples. The number of data points used for the analysis presented here is 5, 000.

- We start with the periodically driven Rössler system [3]:

$$\begin{aligned} \dot{x} &= -y - z + \mu\cos(\omega t) \\ \dot{y} &= x + 0.15y \\ \dot{z} &= 0.4 + z(x - 8.5) \end{aligned} \tag{7}$$

For the driving frequency $\omega = 1.04$ and amplitude $\mu = 0.16$, the periodic forcing locks the frequency of the Rössler system. This can be clearly seen in Figure 3a: the position of the maxima coincide. The value of the recurrence based PS index is $\mathrm{CPR} = 0.862$.

For the parameters $\omega = 1.1$ and $\mu = 0.16$, the periodic forcing does not synchronize the Rössler system. Hence, the joint probability of recurrence is very low, which is reflected in the drift of the corresponding $P(\tau)$ (Figure 3b). In this case, $\mathrm{CPR} = -0.00241$.

- We continue our considerations with the periodically driven Lorenz system:

$$\begin{aligned} \dot{x} &= 10(y - x) \\ \dot{y} &= 28x - y - xz \\ \dot{z} &= -8/3z + xy + \mu\cos(\omega t) \end{aligned} \tag{8}$$

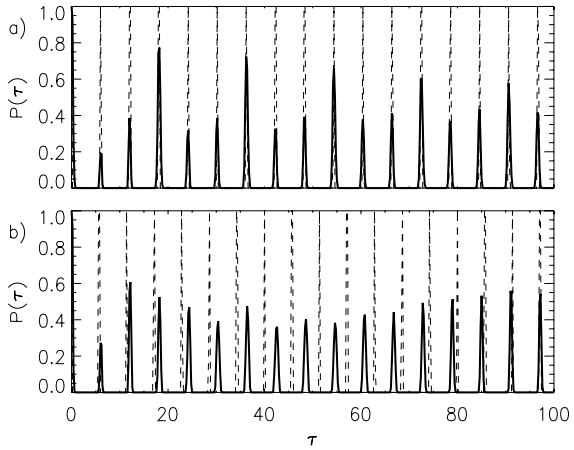

Figure 3. $P(\tau)$ for a periodically driven Rössler (Equations (7)) in PS (a) and in non-PS (b). Solid line: $P(\tau)$ of the driven Rössler, dashed line: $P(\tau)$ of the periodic forcing

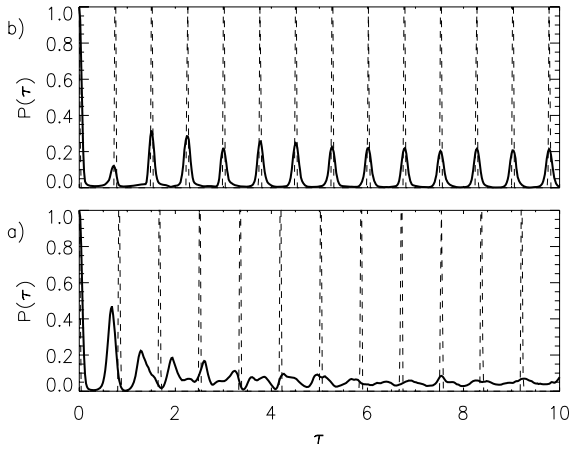

Figure 4. $P(\tau)$ for a periodically driven Lorenz in PS (a) and in non-PS (b). Solid line: $P(\tau)$ of the driven Lorenz, dashed line: $P(\tau)$ of the periodic forcing

In Figure 4a the probabilities of recurrence $P(\tau)$ in the PS case ($\mu = 10$, $\omega = 8.35$) are represented: we see, that the position of the local maxima of the Lorenz oscillator coincide with the ones of the periodic forcing. However, the local maxima are not as high as in the case of the Rössler system, and they are broader. This reflects the effective noise intrinsic in the Lorenz system [4]. Because of this, the phase synchronization is not perfect: an exact frequency locking between the periodic forcing and the driven Lorenz cannot be observed [25]. In this case, we obtain CPR = 0.667. In the non-PS case ($\mu = 10$, $\omega = 7.5$), we get CPR = 0.147 (Figure 4b).

- Now we consider the case of two mutually coupled Rössler systems in the phase coherent regime, i.e., we consider Equation (1) with $a = 0.16$. According to [26], for $\omega_1 = 0.98, \omega_2 = 1.02$ and $\mu = 0.05$ both systems are in PS. We observe that the local maxima of P_1 and P_2 occur at $\tau = n \cdot T$, where T is the mean period of both Rössler systems (Figure 5a). The heights of the local maxima are in general different for both systems if they are only in PS and not in GS, as we will see later. But the positions of the local maxima of $P(\tau)$ coincide. In this case, we obtain CPR = 0.998.

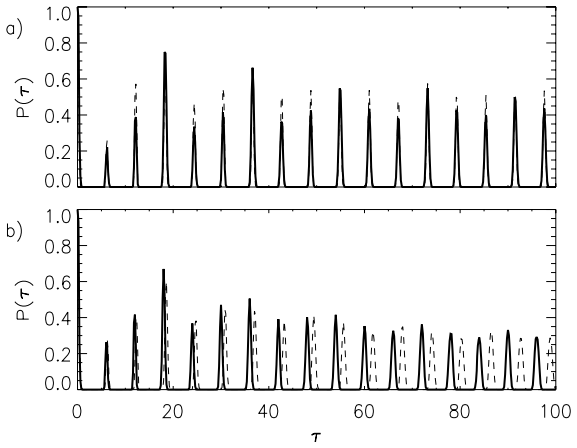

Figure 5. $P(\tau)$ for two mutually coupled Rössler systems (Equations (1)) in phase coherent regime ($a = 0.16$) for $\mu = 0.05$ (a) and for $\mu = 0.02$ (b)

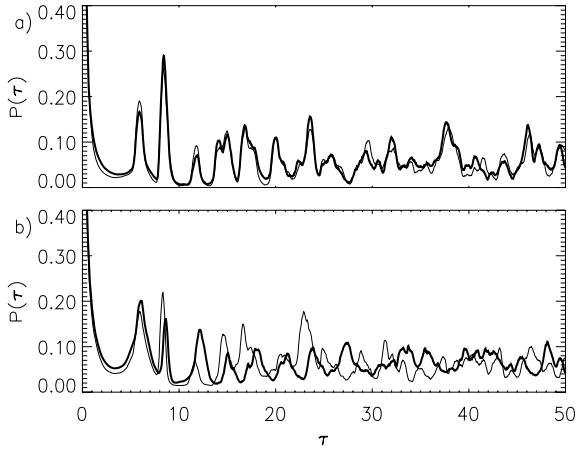

Figure 6. $P(\tau)$ for two mutually coupled Rössler systems (Equations (1)) in funnel regime ($a = 0.2925$) for $\mu = 0.2$ (a) and for $\mu = 0.05$ (b). Bold line: $P_1(\tau)$, solid line: $P_2(\tau)$,

For $\mu = 0.02$ the systems are not in PS and the positions of the maxima of $P(\tau)$ do not coincide anymore (Figure 5b), clearly indicating that the frequencies are not locked. In this case, we obtain $CPR = 0.115$.

- As the last example with simulated data, we analyze the challenging case of two mutually coupled Rössler systems in the funnel regime, i.e., we consider Equation (1) with $a = 0.2925$, $\omega_1 = 0.98$ and $\omega_2 = 1.02$. We analyze two different coupling strengths: $\mu = 0.2$ and $\mu = 0.05$. We observe that the structure of $P(\tau)$ in the funnel regime (Figure 6) is rather different from the one in the phase coherent Rössler system (Figure 5). The peaks in $P(\tau)$ are not as well pronounced as in the coherent regime, reflecting the different time scales that play a relevant role and the broad-band power spectrum of this system. However, we see that for $\mu = 0.2$ the locations of the local maxima coincide for both oscillators (Figure 6a), indicating PS, whereas for $\mu = 0.05$ the positions of the local maxima do not coincide anymore (Figure 6b), indicating non-PS. These results are in accordance with [26].

  In the PS case, we obtain CPR $= 0.988$, and in the non-PS case, CPR $= 0.145$. Note, that the position of the first peak in Figure 6b coincides, although the oscillators are not in PS. This is due to the small frequency mismatch ($|\omega_1 - \omega_2| = 0.04$). However, by means of the index CPR we can distinguish rather well between both regimes.

3.2. Influence of Noise

Dealing with experimental time series, one is always confronted with measurement errors. Hence, it is necessary to analyze the influence of noise on the index CPR for PS.

We consider here additive or observational noise. We use Equation (1) as an example for two different coupling strengths, so that we can compute the deviation which is caused by noise in the nonsynchronized and in the synchronized case.

We add independent Gaussian noise with standard deviation $\sigma_{\text{noise}} = \alpha\sigma_j$ to each coordinate j of the system, where σ_j is the standard deviation of the component j and α is the noise level. In Figure 7, the "corrupted" x-component of the first Rössler subsystem $\tilde{x}_1(t) = x_1(t) + \alpha\sigma_1\eta(t)$, where $\eta(t)$ is a realization of Gaussian noise and $\alpha = 0.8$, is represented. From this figure it is clearly to see, that it is

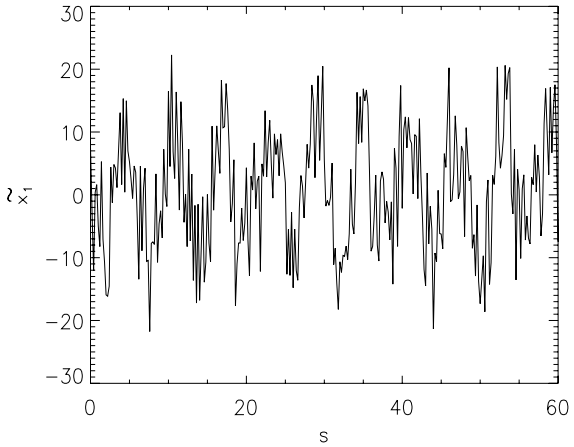

Figure 7. First component x_1 of Equations (1) with 80% independent Gaussian noise (for $\mu = 0.05$). From the figure it is clearly recognizable, that it is difficult to compute the phase by means of, e.g., the Hilbert transformation

difficult to compute the phase by means of, e.g., the Hilbert transformation for such a high noise level without filtering.

The choice of ε for the computation of $P_1(\tau)$ and $P_2(\tau)$ in the presence of noise is automatically taken by fixing a determined recurrence rate RR, i.e., the percentage of recurrence points in the recurrence matrix Equation (4) (see appendix). The results presented below were computed for RR $= 0.1$, but the results are rather independent of the choice of *RR*. However, *RR* should not be chosen too small if the level of noise is very high [27].

In order to compute the index CPR for the noisy oscillators, we calculate first the probabilities of recurrence $P_1(\tau)$ and $P_2(\tau)$ for coupling strengths $\mu = 0.05$ (PS, Figure 8) and $\mu = 0.02$ (non-PS, Figure 9).

We note, that the peaks in $P_1(\tau)$ and $P_2(\tau)$ become lower and broader (Figs. 8b and 9b) compared with the noise free case (Figs. 8a and 9a), as expected. However, despite of the large level of noise, the positions of the local maxima coincide in the PS case, and they drift away in the non-PS

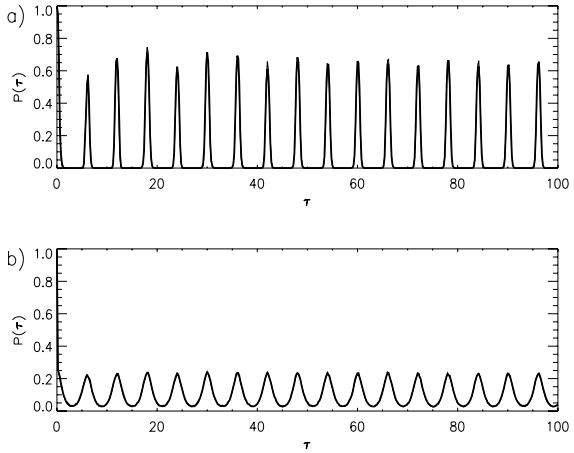

Figure 8. Probabilities of recurrence for two coupled Rössler systems (Equations (1)) in PS ($\mu = 0.05$) without noise (a) and with 80% Gaussian observational noise (b). Bold line: subsystem 1, solid line: subsystem 2. Note that the position of the peaks of $P_1(\tau)$ and $P_2(\tau)$ coincide in both cases, and hence the solid line is hidden by the bold one

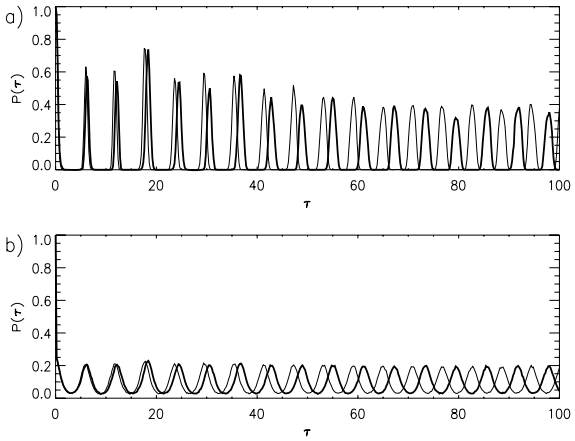

Figure 9. Probabilities of recurrence for two coupled Rössler systems (Equations (1)) in non-PS ($\mu = 0.02$) without noise (a) and with 80% Gaussian observational noise (b). Bold line: subsystem 1, solid line: subsystem 2

Table 1. Index CPR index for PS calculated for two coupled Rössler systems (Equations (1)) with observational noise and without noise, for comparison.

μ	CPR (80% noise)	CPR (0% noise)
0.02 (non-PS)	0.149	0.115
0.05 (PS)	0.998	0.998

case. This a convenient result, because we can still decide whether the oscillators are synchronized or not. This is reflected in the obtained values for the CPR index: with 80% noise, in the PS case the obtained value for CPR is exactly the same with and without noise, and in the non-PS case is nearly the same (see Table 1). This shows that the index *CPR* for PS is very robust against observational noise. Also in the case of dynamical noise we can expect this method to work, due to its averaging.

3.3. Transition to PS

We have seen in the previous sections, that the index CPR clearly distinguishes between oscillators in PS and oscillators which are not in PS. On the other hand, a synchronization index should not only distinguish between synchronized and nonsynchronized regimes, but also indicate clearly the onset of PS.

In order to demonstrate that the recurrence based index fulfills this condition, we exemplify its application in two cases: two mutually coupled Rössler systems in a phase coherent and in a non-phase coherent funnel regime (Equation (1) with $a = 0.16$ respectively a $= 0.2925$). We increase in both cases the coupling strength μ in small steps and compute for each value of μ the index CPR.

On the other hand, in the phase coherent case for a not too large but fixed frequency mismatch between both oscillators and increasing coupling strength, the transition to PS is reflected in the Lyapunov spectrum $(3, 4)$[1]. If both oscillators are not in PS, there are two zero Lyapunov exponents, that correspond

[1] For other cases, e.g., for a fixed coupling strength and decreasing frequency mismatch, or for a large frequency mismatch

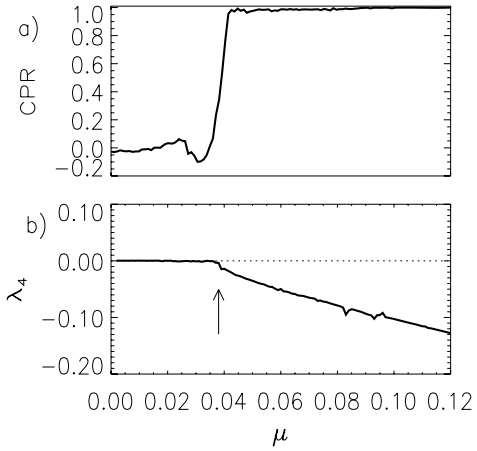

Figure 10. CPR index for PS (a) and λ_4 (b) in dependence on the coupling strength for two mutually coupled Rössler systems in the phase coherent regime. The dotted zero line in (b) is plotted to guide the eye. The arrow indicates the transition of λ_4 to negative values

to the (almost) independent phases. Increasing the coupling strength, the fourth Lyapunov exponent λ_4 becomes negative (see Figure 10b), indicating the onset of PS. Therefore, we compute for our two examples also λ_4 in order to validate the results obtained with CPR.

In Figure 10a, the index CPR is represented for increasing coupling strength μ for the phase coherent case. In Figure 10b, λ_4 is also shown in dependence on μ. By means of CPR, the transition to PS is detected when CPR becomes of the order of 1. We see from Figure 10a, that the transition to PS occurs at approximately $\mu = 0.037$, in accordance with the transition of the fourth Lyapunov exponent λ_4 to negative values (Figure 10b).

Now we regard the more complex case of two coupled Rössler systems in the noncoherent funnel regime, where the direct application of the Hilbert transformation is not appropriate [26]. In Figure 11, the coefficient CPR is represented for this case in dependence on the coupling strength μ. Again, λ_4 is also shown (Figure 11b). First, we note that for $\mu > 0.02$, λ_4 has already passed to negative values (Figure 11b). However, *CPR* is still rather low, indicating that both oscillators are not in PS yet. *CPR* does not reveal the transition to PS until $\mu = 0.18$ (Figure 11a), as found with the modified definition (Equation (3)) of the phase [26]. Furthermore, λ_2 vanishes at $\mu \sim 0.17$ [26], indicating that the amplitudes of both oscillators become highly correlated. Then, according to the index *CPR* and to the definition (Equation (3)) of the phase, the transition to PS occurs after the onset of GS. This is a general result that holds for systems with a strong phase diffusion. For highly non-phase coherent systems, there exists more than one characteristic time scale. Hence, a high coupling strength is necessary in order to maintain the phase locking of both oscillators. Hence, PS is in this case not possible without having a strong correlation in the amplitudes.

3.4. Detection of clusters of PS

Next, we show that our algorithm is also valid for the detection of PS in chains of weakly coupled oscillators. This extension to N oscillators is straightforward: we compute $P_j(\tau)$ for each oscillator j

and increasing coupling strength, the transition to PS is not always reflected in the Lyapunov spectrum [28]

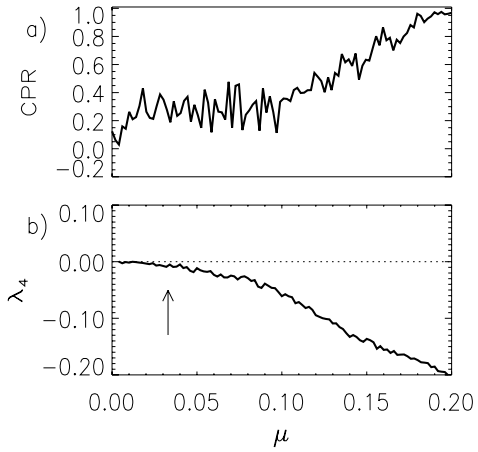

Figure 11. (a) CPR coefficient, (b) λ_4 in dependence on the coupling strength for two mutually coupled Rössler systems in the funnel regime. The dotted zero line in (b) is plotted to guide the eye. The arrow indicates the transition of λ_4 to negative values

(Equation (5)) and their respectively local maxima τ_j^i according to

$$\frac{dP_j(\tau^i)}{d\tau^i} \simeq 0.$$

Then we choose the set of times of local maxima τ_r^i of an arbitrarily chosen (but then fixed) oscillator r as reference and compute $\Delta\tau_j^i = \tau_j^i - \tau_r^i$ for each oscillator j.

Now even clusters of oscillators in PS are easily recognized by means of the mean slope of $\Delta\tau_j^i$ versus i is equal for all oscillators j belonging to the same cluster.

We apply this algorithm to a chain of coupled nonidentical Rössler oscillators with a nearest-neighbor diffusive coupling

$$\begin{aligned}
\dot{x}_j &= -\omega_j y_j - z_j, \\
\dot{y}_j &= \omega_j x_j + a y_j + \mu(y_{j+1} - 2y_j + y_{j-1}), \\
\dot{z}_j &= 0.4 + z_j(x_j - 8.5),
\end{aligned} \tag{9}$$

where the index $j = 1, \ldots, N$ denotes the position of an oscillator in the chain, μ is the coupling coefficient and ω_j corresponds to the natural frequency of each individual oscillator [29]. First, we consider a linear distribution of natural frequencies $\omega_j = \omega_1 + \delta(j-1)$, where δ is the frequency mismatch between neighboring systems. For the coupling strength $\mu = 0.18$ and $\delta = 9 \times 10^{-3}$ we compute $P_j(\tau)$ for $j = 1, \ldots, 50$ and the positions of the local maxima τ_j^i for each oscillator. We choose the oscillator $j = 1$ as reference and compute $\Delta\tau_j^i$ for $j = 1, \ldots, 50$ (Figure 12a). Furthermore, we represent the slope of $\Delta\tau_j^i$ versus i given by a linear regression for $j = 1, \ldots, 50$ in Figure 12b. We detect 9 clusters of oscillators in PS, in accordance with [29]. We have also analyzed this chain of Rössler oscillators with other values of the coupling strength and we obtain the same results as in [29]. Also the computation of the matrix $\mathrm{CPR}^{i,j}$ of the cross-correlation coefficients between $(P_i(\tau), P_j(\tau))$ yields the same results as in [29].

Furthermore, we consider a uniformly distribution of the natural frequencies in the interval $1 < \omega_j < 1.05$. The essential difference with respect to former case, is that for the same mismatch between the

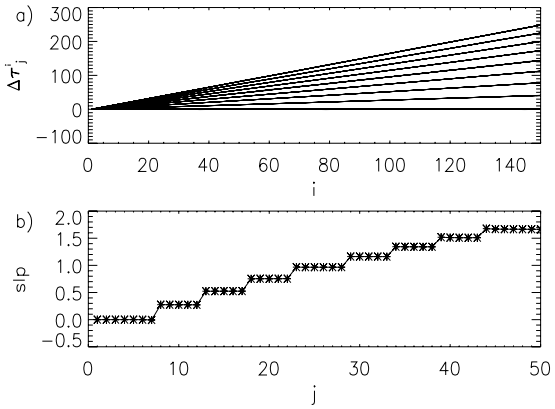

Figure 12. (a) Difference between the local maxima of the probability of recurrence for a chain of 50 Rössler oscillators diffusively coupled for $\mu = 0.18$ and $\delta = 9 \times 10^{-3}$. (b) Slope of $\Delta\tau^i_j$ versus i for $j = 1, \ldots, 50$ with $\mu = 0.18$ and $\delta = 9 \times 10^{-3}$.

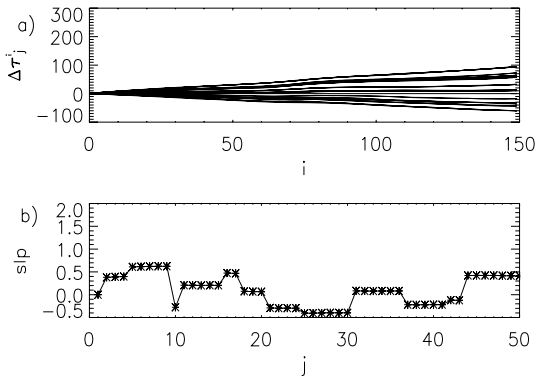

Figure 13. (a) Difference between the local maxima of the probability of recurrence for a chain of 50 Rössler oscillators diffusively coupled for $\mu = 0.02$ and natural frequencies uniformly random distributed. (b) Slope of $\Delta\tau^i_j$ versus i for $j = 1, \ldots, 50$ with $\mu = 0.02$.

largest and the smallest of ω_j, clusters of synchronization appear for considerably lower values of the coupling μ. We detect about 10 clusters for $\mu = 0.02$ (Figure 13).

3.5. Application to a population of chaotic electrochemical oscillators

In order to show the applicability of the method to an experimental system, we analyze data from a population of 64 nonidentical chaotic electrochemical oscillators with weak global coupling. The electrochemical system is the electrodissolution of Ni in 4.5 mol/l sulfuric acid solution (see [30] for the details of the experiment). The electrochemical oscillators are electrically coupled with a combination of one series (R_s) and 64 parallel (R_p) resistors; a global coupling parameter can be defined as $\mu = R_s/(R_p N)$, where $N = 64$ is the number of elements.

We present here the results for three different coupling strengths: without ($\mu = 0.0$), with small ($\mu = 0.05$), and with relatively strong ($\mu = 0.1$) coupling. Without coupling the oscillators have an approximately unimodal frequency distribution with a mean frequency of 1.219 Hz and a standard deviation of 18 mHz.

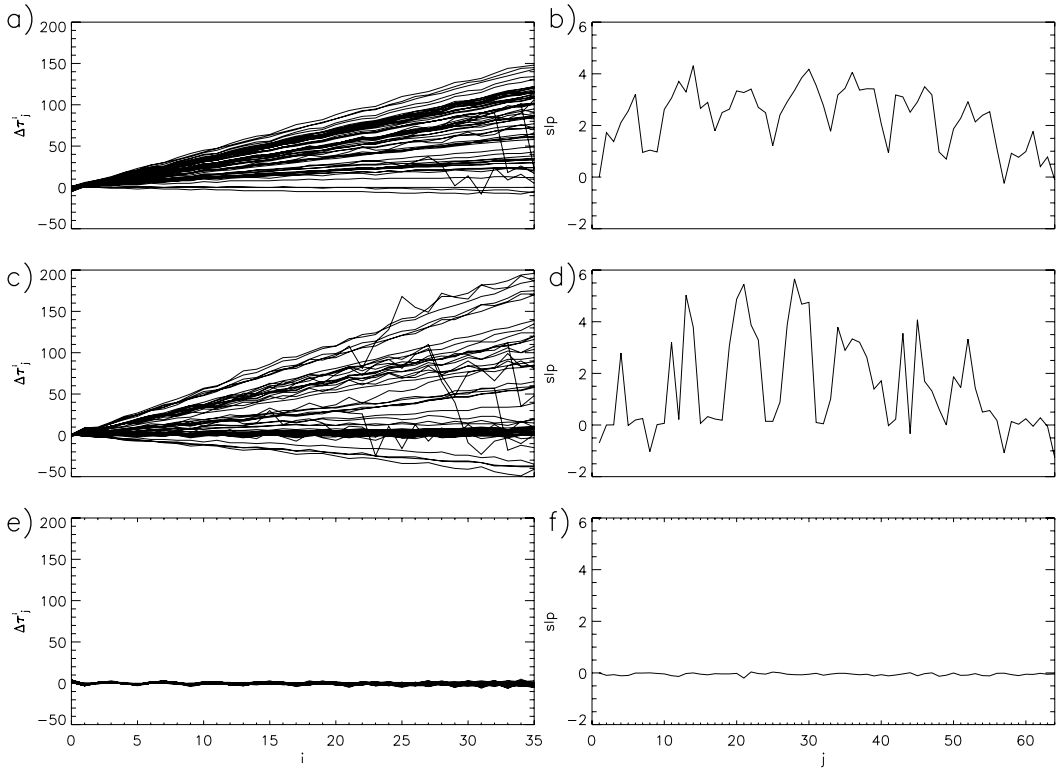

Figure 14. (a) Difference between the local maxima of the probability of recurrence $\Delta\tau_j^i$ versus i for a population of 64 chaotic electrochemical oscillators and slope of $\Delta\tau_j^i$ versus j for $j = 1, \ldots, 64$ (j denotes the oscillator and i the time). (a) and (b) for coupling strength $\mu = 0$, (c) and (d) for $\mu = 0.05$, (e) and (f) for $\mu = 0.1$.

After computing $P_j(\tau)$ for $j = 1, \ldots, 64$ we calculate $\Delta\tau_j^i$, where the oscillator $r = 1$ was chosen as reference (Figure 14). We note that in the absence of coupling the slope of $\Delta\tau_j^i$ versus i is different for each oscillator (Figs. 14a and b). Increasing the coupling strength to $\mu = 0.05$ we observe a main group of oscillators that have almost slope 0, but still many of them are spread out (Figs. 14c and d). If we increase further the coupling strength to $\mu = 0.1$, we observe that all 64 oscillators have an approximately vanishing slope, and therefore they are in PS (Figs. 14e and f), as reported in [30].

4. Conclusions

In this paper we have presented two different approaches to overcome the problem of defining the phase in the case of noncoherent oscillators. The first one is based on the general idea of curvature of an arbitrary curve, and yields a new definition of the phase, that is applicable to a broad class of oscillators, not only to coherent ones. The second approach that we have presented, is an indirect one. It does not compute the phase explicitely, but it detects CPS by means of the joint probability of recurrence in phase space. This method can be also applied to detect CPS in noncoherent oscillators and it is additionally very robust against noise and can be easily implemented. Further, it also allows the detection of clusters of phase synchronized oscillators in distributed systems.

Acknowledgements

This work was supported in part by the National Science Foundation under grants CTS-0000483 and CTS-0317762, the "DFG priority program 1114" and "Internationales Promotionskolleg Computational Neuroscience of Behavioral Cognitive Dynamics". G.O. and M.I. also acknowledge financial support of RFBR (project N 03-02-17543).

Appedix A: The choice of ϵ

A.1.

By computing the recurrence matrix (Equation (4)) or measures based on it, the question arises, which values of ε one should consider. As each system has its own amplitude, which may differ from one system to another one, the choice will be different for each case and it is subjected to some arbitrariness. In order to overcome this problem, we can fix the value of the recurrence rate *RR*, i.e., the percentage of recurrence or black points in the matrix, defined as

$$RR = \frac{1}{N^2} \sum_{i,j=1}^{N} \Theta(\varepsilon - ||\vec{x}_i - \vec{x}_j||) \tag{A.1}$$

As the *RR* is normalized, it is convenient to fix its value and then calculate the corresponding ε. This can be done by the following algorithm:

1. Compute the distances between each pair of vectors $i = 1, \ldots, N$ and $j = 1, \ldots, i$. Then we obtain the series d_l with $l = 1, \ldots, N^2/2$ (because of the symmetry of the recurrence matrix, we consider only the half of the it. Actually the length of the series of the distances is equal to $N^2/2 - N$, but for large N, we can write $N^2/2$.).
2. Sort the distances d_l in ascending order and denote the rank ordered distances by $\tilde{d}_l$, with $l = 1, \ldots, N^2/2$.
3. For a fixed *RR* the corresponding ε is then given by $\tilde{d}_m$, with $m = RR\frac{N^2}{2}$. For example, if $RR = 0.01$, then $\varepsilon = \tilde{d}_{0.01N^2/2}$. We then know that 1% of the distances are less or equal than ε, and hence $RR = 0.01$.

Like this, we avoid the arbitrariness of choosing appropriate values for ε and we can apply the same procedure to all systems. Simulations show that choosing values of *RR* approximately between 1 and 10% do not change the results of the synchronization analysis with the recurrence based method.

References

1. Rosenblum, M., Pikovsky, A., and Kurths, J., 'Phase synchronization of chaotic oscillators', *Physical Review Letters* **76**, 1996, 1804–1807.
2. Pikovsky, A., Rosenblum, M., Osipov, G., and Kurths, J., 'Nonlinear Phenomena, Phase synchronization of chaotic oscillators by external driving', *Physica D* **104**, 1997, 219–238.
3. Pikovsky, A., Rosenblum, M., and Kurths, J. *Synchronization*, Cambridge Nonlinear Science Series 12, 2001.
4. Boccaletti, S., Kurths, J., Osipov, G. V., Valladares, D., and Zhou, C., 'The synchronization of chaotic systems', *Physics Reports* **366**, 2002, 1–101.

5. Elson, R. C., Selverston, A. I., Huerta, R., Rulkov, N. F., Rabinovich, M. I., and Abarbanel, H. D. I., 'Synchronous behavior of two coupled biological neurons', *Physical Review Letters* **81**, 1998, 5692–5695.
6. Tass, P., Rosenblum, M. G., Weule, J., Kurths, J., Pikovsky, A., Volkmann, J., Schnitzler, A., and Freund, H.-J., 'Detection of n:m phase locking from noisy data: Application to magnetoencephalography', *Physical Review Letters* **81**, 1998, 3291–3294.
7. Ticos, C. M., Rosa, E., Jr., Pardo, W. B., Walkenstein, J. A., and Monti, M., 'Experimental real-time phase synchronization of a paced chaotic plasma discharge', *Physical Review Letters* **85**, 2000, 2929–2932.
8. Makarenko, V. and Llinas, R., 'Experimentally determined chaotic phase synchronization in a neuronal system', in *Proceedings of the National Academy of Sciences of the United States of America*, **95**, 1998, 15747–15752.
9. Blasius, B., Huppert, A., and Stone, L., 'Complex dynamics and phase synchronization in spatially extended ecological systems', *Nature* **399**, 1999, 354–359.
10. Schäfer, C., Rosenblum, M. G., Kurths, J., and Abel, H.-H., 'Heartbeat synchronized with ventilation', *Nature* **392**, 1998, 239–240.
11. DeShazer, D. J., Breban, R., Ott, E., and Roy, R., 'Detecting phase synchronization in a chaotic laser array', *Physical Review Letters* **87**, 2001, 044101.
12. Boccaletti, S., Allaria, E., Meucci, R., and Arecchi, F.T., 'Experimental characterization of the transition to phase synchronization of chaotic CO2 laser systems', *Physical Review Letters* **89**, 2002, 194101
13. Kiss, I. Z. and Hudson, J. L., 'Phase synchronization and suppression of chaos through intermittency in forcing of an electrochemical oscillator', *Physical Review E* **64**, 2001, 046215.
14. Fisher, G. *Plane algebraic curves*, American Mathematical Soceity, Providence, RI, 2001.
15. Sparrow, C. *The Lorenz Equations: Bifurcations, Chaos, and Strange Attractors*, Springer-Verlag, Berlin, 1982.
16. Madan, R. N. *Chua circuit: A paradigm for chaos*, World Scientific, Singapore, 1993.
17. Lauterborn, W., Kurz, T., and Wiesenfeldt, M. *Coherent Optics. Fundamentals and Applications*. Springer-Verlag, Berlin, Heidelberg, New York, 1993.
18. Kiss, I. Z., Lv, Q., and Hudson, J. L., 'Synchronization of non-phase-coherent chaotic electrochemical oscillations', *Physical Review E* **71**, 2005, 035201(R).
19. Chen, J. Y., Wong, K. W., Zheng, H. Y., and Shuai, J. W., 'Intermittent phase synchronization of coupled spatiotemporal chaotic systems', *Physical Review E* **64**, 2001, 016212.
20. Poincaré, H., 'Sur le problème des trios corps et les equations de la dynamique', *Acta Mathmatica* **13**, 1890, 1–27.
21. Eckmann, J. P., Kamphorst, S. O., and Ruelle, D., 'Recurrence plots of dynamical systems', *Europhysics Letters* **4**, 1987, 973–977.
22. Thiel, M., Romano, M. C., and Kurths, J., 'How much information is contained in a recurrence plot?', *Physics Letters A* **330**(5), 2004, 343–349.
23. Thiel, M., Romano, M. C., Read, P., and Kurths, J., 'Estimation of dynamical invariants without embedding by recurrence plots', *Chaos* **14**(2), 2004, 234–243.
24. Marwan, N., Trauth, M. H., Vuille, M., Kurths, J., 'Comparing modern and Pleistocene ENSO-like influences in NW Argentina using nonlinear time series analysis methods', *Climate Dynamics* **21**(3–4), 2003, 317–326.
25. Park, E.-H., Zaks, M., and Kurths, J., 'Phase synchronization in the forced Lorenz system', *Physical Review E* **60**, 1999, 6627–6638.
26. Osipov, G. V., Hu, B., Zhou, C., Ivanchenko, M. V., and Kurths, J., 'Three types of transitions to phase synchronization in coupled chaotic oscillators', *Physical Review Letters* **91**, 2003, 024101.
27. Thiel, M., Romano, M. C., Kurths, J., Meucci, R., Allaria, E., and Arecchi, F. T., 'Nonlinear Dynamics, Influence of observational noise on the recurrence quantification analysis', *Physica D* **171**(3), 2002, 138–152.
28. Romano, M. C., Thiel, M., Kurths, J., and von Bloh, W., 'Multivariate recurrence plots', *Physics Letters A* **330**, 2004, 214–223.
29. Osipov, G. V., Pikovsky, A., Rosenblum, M., and Kurths, J., 'Phase synchronization effects in a lattice of nonidentical Rössler oscillators', *Physical Review E* **55**, 1997, 2353–2361.
30. Kiss, I. Z., Zhai, Y., and Hudson, J. L., 'Collective dynamics of chaotic chemical oscillators and the law of large numbers', *Physical Review Letters* **88**, 2002, 238301.